Age, evolution and regional setting of the Palaeoproterozoic Umba igneous suite in the Kolvitsa–Umba zone, Kola Peninsula: Constraints from new geological, geochemical and U–Pb zir…

Article *in* Precambrian Research · January 2001

DOI: 10.1016/S0301-9268(00)00114-5

CITATIONS
32

READS
74

7 authors, including:

N. L. Alexeev
A.P. Karpinsky Russian Geological Research Institute
19 PUBLICATIONS **98** CITATIONS
SEE PROFILE

Ekaterina Salnikova
Russian Academy of Sciences
210 PUBLICATIONS **3,989** CITATIONS
SEE PROFILE

ELSEVIER

Precambrian Research 105 (2001) 247–267

Precambrian Research

www.elsevier.com/locate/precamres

Age, evolution and regional setting of the Palaeoproterozoic Umba igneous suite in the Kolvitsa–Umba zone, Kola Peninsula: constraints from new geological, geochemical and U–Pb zircon data

Viktor Glebovitsky [a,*], Mogens Marker [b], Nikolay Alexejev [a], David Bridgwater [c], Irina Sedova [a], Ekaterina Salnikova [a], Natalia Berezhnaya [a]

[a] *Institute of Precambrian Geology and Geochronology, RAS, St Petersburg, Russia*
[b] *Geological Survey of Norway, Box 3006, N-7002 Trondheim, Norway*
[c] *Geological Museum, Copenhagen University, Oster Voldgade 5-7, DK-1350 Copenhagen K, Denmark*

Received 20 August 1999; accepted 1 November 1999

Abstract

The Umba igneous complex consists of an enderbite–charnockite suite, including porphyritic variety of charnockites, and a porphyritic granite. Both are intruded by irregular veins or minor bodies of later reddish granite. The porphyritic charnockites locally contains abundant xenoliths of country rocks and its contamination by sedimentary material is expressed by a minor content of garnet, that increases in amount in areas with sedimentary inclusions. The Umba igneous complex and the Umba block metasediments were deformed together during two episodes of deformation. The first one was a major episode of thrusting with the formation of a penetrative shear foliation (S_1), which dips gently eastwards, and a gently SE-plunging lineation. Coeval with this thrusting, the boundary between the Umba block and the Poriya Guba series in the southeast developed as a strike-slip shear zone, that juxtaposed the two blocks along a tectonic melange zone. The S_1-shearing deformed the enderbite–charnockite suite, and probably also the porphyritic granite, into plate-like, eastward-dipping bodies. Predating the shearing, the metasediments underwent high-grade metamorphism and anatexis leading to a high degree of partial melting. This anatexis is also found in the enderbite–charnockite suite, but in a much smaller scale and mainly in the marginal parts of the bodies. The second episode of deformation formed narrow localized extensional shear zones (S_2), which are developed in all rock units. The S_1-shearing in the tectonic melange zone occurred under high-pressure metamorphism during cooling at constant pressure ($T = 806–818$°C, $P = 9.3–9.5$ kbar) and then at decreasing pressure due to tectonic uplift. Both seem to have gone through the same deformation events as the metasediments. The S_2-extension occurred under decompression ($P = 7.5–8.0$ kbar, $T = 860–840$°C) caused by uplift or tectonic erosion of the thrust pile. Though indistinguishable in the field the enderbite–charnockite suite form a discontinuous suite with a trondhjemitic trend for the former, and a calc–alkaline trend for the latter. Geochemical study shows that the charnockite group is more strongly differentiated than the enderbite group and that magmatic differentiation in the charnockites were

* Corresponding author.

PII: S0301-9268(00)00114-5

controlled by K-feldspar fractionation. The enderbites, on the other hand, lack differentiation and are considered to have crystallized rapidly from its magma source. The charnockites came from a different source that, judging from the high K/Rb ratio, formed at a deeper crustal level than the enderbites. Both members of the enderbite–charnockite suite formed due to subduction in an island arc setting, and Sm–Nd model ages of 2.1–1.9 Ga indicate that the Palaeoproterozoic suite has a juvenile character. Conventional U-Pb zircon dating of the porphyritic charnockite has given discordant ages of 1912.5 ± 7.7 Ma, 1949 ± 7 Ma and 1966 ± 9. Our preferred interpretation is that the 1912.5 ± 7.7 Ma age represents the age of intrusion, or maximum intrusion age of the charnockites, and that the 1949 ± 7 Ma and 1966 ± 9 Ma ages for the abraded type represent ages or mixed ages of inherited zircons from the contaminating Umba block metasediments. The youngest detrital zircons in these metasediments have similar ages. Their source could have been early magmatic arc intrusives, which were eroded shortly after their formation. If the Umba metasediments were deposited in a magmatic arc setting their initial deformation in an evolving arc may have provided the necessary heat flow for anatexis and high-grade peak metamorphism of the metasediments. Therefore, the intrusions of the enderbite–charnokite suite during the later evolution of the magmatic arc could have post-dated the peak of metamorphism, but still pre-date collision and thrusting leading to tectonic telescoping of the units, and thus explain the lower metamorphic grade in the Umba igneous complex compared to the metasediments. If the 1912.5 ± 7.7 Ma age represents the maximum time of intrusion, the true intrusion age might be slightly younger.

Keywords: Umba igneous complex; Porphyritic granite; Xenoliths

1. Introduction

The Umba igneous complex consists of enderbite to charnockite and porphyritic granite which intruded granulite facies paragneisses of the Umba block at the eastern end of the Palaeoproterozoic Kolvitsa-Umba zone of high-grade gneisses, outcropping on the north coast of the White Sea (Fig. 1). This belt is generally assumed to form the southeasternmost extension of the Lapland Granulite Belt, which forms the core of the southeast-trending Palaeoproterozoic Lapland–Kola orogen in the northern Baltic Shield (Bridgwater et al., 1991). The age and petrogenesis of the Umba igneous complex are key problems in understanding the evolution of the Kolvitsa–Umba zone, and its significance and position in the orogenic collage. The complex is the youngest magmatic suite in the Kolvitsa–Umba zone emplaced during a convergent stage in the orogenic evolution. Tectonic collision and destruction succeeded a prolonged period of extensional tectonics in the shield which started c. 2.45 Ga, when numerous mafic to ultramafic layered intrusions were emplaced during initial crustal rifting in the Kola Peninsula, Northern Finland and Northern Karelia (Frisch et al., 1995; Mitrofanov et al., 1995).

In the northwestern part of the Lapland–Kola orogen, rifting was followed by crustal separation and ocean formation, with deposition of thick piles of turbiditic sediments along the margins of the continents (Barbey et al., 1984). Around 2.0 Ga the tectonic regime shifted to convergence with the formation of subduction-related magmatic arcs (Barling et al., 1997; Daly et al., 1997). Continent–continent collision ended this tectonic regime at ca 1.9 Ga resulting in dismembering of rock units in the Lapland–Kola orogen during thrust translation onto the Archaean Karelian–Belomorian craton in the south (Barbey et al., 1984; Marker, 1988; Glebovitsky, 1993; Korja et al., 1996).

In the Kolvitsa–Umba zone, in the southeastern part of the Lapland–Kola orogen, the tectonic configuration differs somewhat from the northwestern part, such as greater involvement of strike-slip movement (Balagansky et al., 1994), though the timing of events appears to be in the same general range as in the northwest. The Umba block, to the southeast in the Kolvitsa–Umba belt, consists of high-grade metasediments and an igneous suite of enderbite–charnockite

similar to those in the Lapland Granulite Belt. The new geological and isotope-geochronological data from the Umba igneous suite are therefore important, since they give a better understanding of particularly the convergent stage in the tectonic evolution of the southeastern Lapland–Kola orogen and thereby improve the possibilities for correlation with other parts of the orogen.

2. Regional setting

The Umba igneous suite is interlayered with metasediments in the southeastern end of the Kolvitsa–Umba zone of high-grade rocks (Fig. 1), which outcrop along the northeasternmost margin of the Belomorian structural domain exposed along the northern shore of the Kandalaksha Bay, White Sea. From west to east, this high-grade zone consists of six major lithological components.

- Late Archaean, 2.72–2.74 Ga (Bogdanova and Bibikova, 1993; Bibikova et al., 1995a,b, 1996) Belomorian gneisses dominated by tonalitic and dioritic orthogneisses.
- Early Palaeoproterozoic Kandalaksha series, dominantly metavolcanic rocks of tholeiitic or calc–alkaline compositions which are interlayered with minor metasedimentary rocks, including graywacke turbidites and conglomerates. These are intruded by thin tonalitic sheets. Andesites from the volcanic suite have given U–Pb zircon ages of c. 2.47 Ga which are interpreted to represent magmatic crystallization (Balagansky et al., 1998). This is supported by whole rock Rb–Sr ages from metavolcanic rocks (Balagansky et al., 1998) strongly suggesting that the formation of the Kandalaksha series occurred at c. 2.47 Ga.
- Kolvitsa massif of gabbro-anorthosites which has U/Pb zircon ages of $2462 + 7/-6$ Ma (Frisch et al., 1995) and 2450 ± 7 Ma (Mitro-

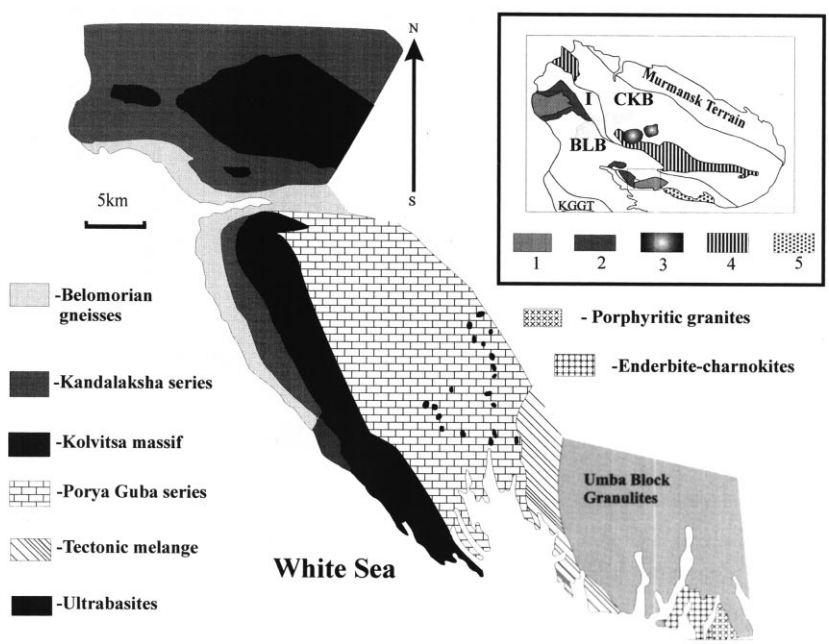

Fig. 1. Geological map of the Kolvitsa–Umba Zone (simplified after Mitrofanov et al., 1995). Insert-major structural domains of Kola Peninsula (after Balagansky and Glaznev): 1, 2 — the Lapland Granulite Belt: 1 — Lapland and Umba granulites; 2 — volcano-sedimentary suits; 3 — alkaline intrusives; 4 — Petchenga-Imandra-Varzuga Belt; 5 — Riphean cover. KGGT, Karelian Granite-Greenstone Terrain; BLB, Belomorian-Lapland Belt; I, Innary Block; CKB, Central Kola Block.

fanov et al., 1995). The massif is cut by dioritic sheets one of which has been dated at 2436 ± 6 Ma (Kaulina, 1996) and by a complex swarm of basic dikes intruded between 2.35 and 2.45 Ga. Comparable mafic dikes intrude volcanic rocks of the Kandalaksha series (Balagansky et al., 1986).

- Poriya Guba supracrustal suite of mainly metavolcanic origin and tholeiitic to andesitic composition. The relative age of this suite is not easily determined as it is bounded by shear zones. However, the data presented by Kaulina (1996) suggest that protoliths to enderbitic gneiss members that are interlayered with mafic rocks may be as old as c. 2.50 Ga.
- Umba block suite of strongly migmatised granulite facies metasediments with minor basic components. The metasediments yield $T(_{DM})$Sm–Nd model ages between 2.125–2.424 Ga (Daly et al., 1997), but contain detrital zircon grains with Pb–Pb ages ranging from 3.7 to 2.2 Ga that indicate both Archaean and Palaeoproterozoic crustal sources (Bridgwater et al., in press). From the range in DM ages and the known presence of Archaean zircons it can be argued that deposition must have occurred later than 2.1 Ga.
- An enderbite–charnockite–porphyritic granite igneous suite in the Umba series, yielding T_{DM} Sm–Nd model ages ranging between 1.9 and 2.1 Ga. (Timmerman and Balagansky, 1994) suggesting a maximum intrusion age of < 2.1 Ga. U–Pb age determinations by Pushkariov et al. (1978) on zircon, monazite and orthite yield a 2150 ± 45 Ma concordia intercept age. A correction of the different decay constants used in 1978 would bring the age more in line with the Sm–Nd model ages of 1.9 Ga.

3. Geology of the Umba-Poriya Guba area

The Umba-Poriya Guba area was investigated during the present study. The field investigations were focused on the Umba block, consisting of the last two lithological components mentioned above, and involved geological mapping of the coastal zone, metamorphic and structural studies, and sampling for geochemical, isotope and geochronological work.

The rocks are divided into the Umba block series comprising the Umba supracrustal suite which is intruded by the Umba igneous complex, and the Poriya Guba series (Fig. 2). The boundary between the two is a major shear zone developed as a tectonic melange (Balagansky and Kozlova, 1987; Balagansky et al., 1994) on the Poriya Guba series side. While the metasedimentary suite of the Umba block shows a well-layered mylonitic structure along the contact, the Poriya Guba series consists of variably deformed, rather fine-grained gray gneisses with bands and inclusions of mafic to intermediate rocks. A planar-banded high-strain structure is most prominent near the contact with the Umba block metasediments, while strain decreases westwards. Here the gray gneisses contain lenses or layers of folded, anatectic, garnet–sillimanite-bearing metasediments similar to those in the Umba block. A tectonic melange is developed on the east shore of Poriya Guba. The melange shows a high degree of stretching parallel to the general gently SE-plunging lineation, outlined by cigar-shaped bodies of amphibolite, which formed due to strike-slip movement.

The Umba block consists of high-grade metasediments in the west and dominantly plutonic rocks of the Umba igneous complex in the east (Fig. 2). The latter is further subdivided into a western enderbite–charnockite suite, where a separate body of their porphyritic variety was distinguished, and an eastern porphyritic granite, where charnockites compose the marginal part of a large massif (Vinogradov and Vinogradova, 1975). The garnet–sillimanite-bearing metasediments show high degrees of anatectic melting, commonly amounting to more than 50% by volume. Detrital zircons from one sample show that the metasediments were derived from a mixed Archaean–Palaeoproterozoic source and that deposition occurred later than 2.1 Ga (Bridgwater et al., in press). The Umba block metasediments usually show a well-developed, planar banded, ductile mylonitic foliation, post-dating anatexis that dips gently eastwards beneath the Umba igneous complex. A penetrative stretching lineation consistently plunge gently SE-wards and

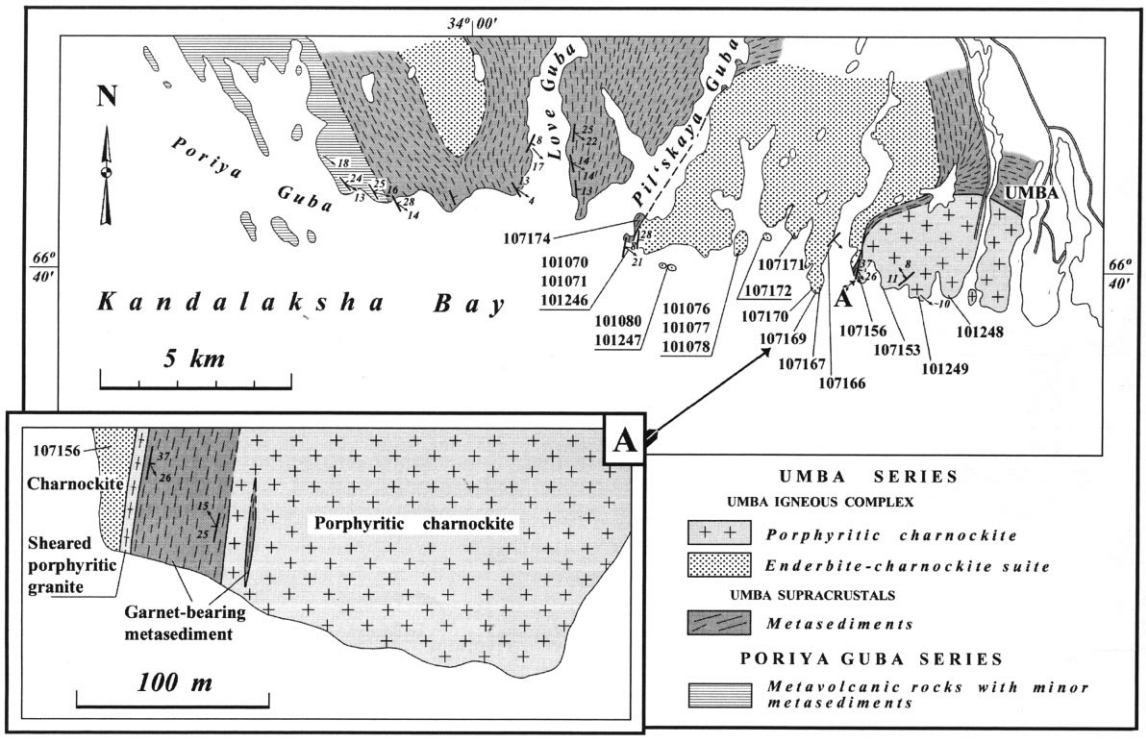

Fig. 2. Geological map of the Poriya Guba-Umba area with localities of samples.

kinematic strain indicators indicate according to Balagansky et al. (1994) top to the SE translation, and sometimes in the opposite direction. A younger extensional shear fabric overprints this mylonitic foliation, localized in steeper E- or W-dipping, ductile minor shears that trend roughly N–S with a dominating down-throw to the east. Some of these form conjugate sets showing this E–W extension as east of the mouth of Pil'skaya Guba. Similar extensional faults were observed in the tectonic melange zone east of the Poriya Guba bay.

The enderbite–charnockite-porphyritic granite suite of the Umba igneous complex occur as discrete bodies that at least at the coast contain a thin panel of Umba block metasediment at the margin (Fig. 2 and insert figure A). The enderbite–charnockite suite in the west consist of medium-grained, homogeneous, rather dark brownish gray granitoids and porphyritic variety of charnockites that show a various degree of deformation. They range in composition from tonalite to granodiorite. There appears to be a gradual variation in composition and it was not possible to make any subdivision of the suite in the field. The enderbite–charnockite suite contains a few irregular minor bodies of late reddish granite (samples 107153 and 101078), which is considered here as the member of charnockite suite.

The main part of the enderbite–charnockite suite usually shows only a weak foliation but near the margins of the Umba metasediments the foliation is more developed. At the mouth of Pil'skaya Guba, an increasing strain gradient over a few hundred meters can be observed towards the mylonitic banded metasediments. Near the boundary, the enderbite–charnockite suite shows a distinct, gently E-dipping planar (shear-induced) foliation, which conforms with the mylonitic foliation in the metasediments to the west. Weakly foliated enderbite–charnokite commonly comprise orthopyroxene as the main mafic mineral,

which probably has igneous origin. Orthopyroxene is partly replaced by biotite or hornblende. At the boundary with the metasediments only rare relics of orthopyroxene overgrown by biotite are encountered in the enderbite–charnokites. Also in the area near the boundary with the porphyritic granite, the enderbite–charnockite suite shows a distinct foliation that dips gently eastwards (Fig. 2), indicating that the suite forms a deformed, gently eastward-dipping sheet-like body, estimated to be c. 3.5 km thick. The enderbite–charnockite at the boundary to the porphyritic granite itself show a strong foliation.

The enderbite–charnockite body does not usually show signs of anatexis, but near the foliated western boundary it contains scattered conformable, 2–4 cm wide, light gray schlieren and veins of quartz–feldspar composition, which could be interpreted as due to anatexis at the margin (introduction of water from nearby metasediments) of the otherwise dry charnockitic complex. The Umba block metasediments, particularly those between the Lov Guba and Pil'skaya Guba bays, contain scattered, one to a few dm thick layers or fishes of more fine-grained dark gray enderbitic–charnockitic rock of similar composition as the main enderbite–charnockite body (sample 107174). These are clearly deformed and concordant with the mylonitic foliation in the metasediments, indicating that following the enderbite–charnockite igneous suite underwent the same shear events as the metasediments.

The porphyritic variety of chrnockites outcrops in a 4 km size body southwest of Umba (Fig. 2), and is marginal part of much larger occurrences the porphyritic granites in the area southeast of Umba. The porphyritic charnockuite is a homogeneous, medium grained, mainly orthopyroxene-bearing gray rock with somewhat rounded, 2–6 cm long phenocrysts of gray to pinkish alkali feldspar. The phenocrysts makes up 10–20% of the rock and are usually unoriented. In many cases orthopyroxene is partly replaced by biotite, and in strongly sheared parts at the boundary with the enderbite–charnockites biotite replacement is complete. The porphyritic charnockite usually contains a few, <5 mm large bright red garnets and some scattered small fishes of fine-grained gray metasediment. The central and western parts of the body are locally rich in 0.1–2 m thick layers or fishes of rather fine-grained garnet-bearing metasediments that show few signs of anatexis. Where rich in sedimentary inclusions, the garnet content in the porphyritic charnockite increases significantly. A c. 60 m thick layer of anatectic garnet-bearing metasediment occurs close to the boundary with the enderbite (insert map A in Fig. 2). The garnet content bears evidence of variable contamination of the porphyritic charnockite by sedimentary material in most part of the body. The less contaminated eastern part of the body was sampled for geochronology (sample 101249 represents the most mafic variety of porphyritic charnockite).

The porphyritic charnockite is usually quite homogeneous, but in areas, such as in the central part, with many sedimentary inclusions, the granite develops foliation, that dips gently in various directions. The porphyritic charnockite is also well-foliated along the conformable shear contact with the charnockitic rocks in the west (insert map A Fig. 2). However, where mineral lineations could be measured, they always plunge gently towards the SE or NW parallel with the stretching lineation in the Umba metasediments. This indicates that the porphyritic charnockite may have experienced the same events of shear deformation as the metasediments and the enderbite–charnockite suite.

4. Metamorphic evolution of the Kolvitsa–Umba zone

The metamorphic and structural evolution of the Kolvitsa–Umba zone is complex and the subject of ongoing research. With the exception of the amphibolite facies Kandalaksha series the main units have been affected by at least one phase of medium to high pressure granulite facies metamorphism (Glebovitsky, 1997). The youngest of these developed in the period 1.9–1.95 Ga. and affected both the western Kolvitsa belt (c. 1906 Ma, Frisch et al., 1995) and the eastern Umba block paragneisses, and most likely also its granitoids. This phase of high-grade metamorphism is

interpreted as related to crustal collision during the formation of the Lapland–Kola orogen and is broadly contemporaneous with metamorphism in the Lapland Granulite Belt 100 km further to the northwest (Tugarinov and Bibikova, 1980; Glebovitsky, 1993, 1997).

There is considerable evidence that the igneous complexes west of the Poriya Guba series, the Kolvitsa gabbro-anorthosite massif and associated dioritic intrusions and basic dikes, experienced an earlier granulite facies event, related to deformation before c. 2.4–2.3 Ga. (Alexejev, 1997). Our preferred interpretations are that part of the Kolvitsa massif either crystallized at depth under granulite facies conditions or was brought tectonically down to a deep level in the crust shortly after its formation. In any case, part of the massif became strongly deformed under high-grade metamorphic conditions before or during basic dike injection, which started at c. 2.43 Ga., and possibly could have lasted for more than 100 million years (Glebovitsky et al., 1997; Balagansky et al., 1999, in press).

The Umba block granulite facies metasediments, which are interpreted as the southeastern extension of the Lapland Granulite Belt, are separated from the Kolvitsa igneous massif and the Kandalaksha series in the west by the metavolcanic suite of the Poriya Guba series. The contact between the Poriya Guba and Umba block metasediments further east is a spectacular tectonic melange which is up to 5–6 km wide (Balagansky and Kozlova, 1987; Balagansky et al., 1994). The boundary between the Umba series and the tectonically underlying Poriya Guba rocks has been interpreted as a major thrust zone (Kozlova et al., 1991; Glebovitsky, 1993; Balagansky et al., 1994). The formation of the tectonic melange showing dominantly dextral strike-slip movements, was coeval with S_1-shearing in the metasediments, that resulted in the development of a WNW–ESE-trending, subhorizontal stretching lineation in both the tectonic melange zone and the Umba block metasediments. The S_1-shearing was accompanied by crystallization of orthopyroxene-sillimanite assemblages as replacements of Mg–Gar + Al–Opx (Kozlova et al., 1991; Alexejev, 1997) in the northwestern part of the tectonic melange. This is thought to have been achieved by cooling at constant pressure of the tectonic melange zone rocks (Fig. 3a). TWEEQU calculations for Grt–Opx–Sill assemblages give $T = 806–818$°C and $P = 9.3–9.5$ kbar. However, Gar–Spl–Qtz assemblages developed in the central part of the tectonic melange zone indicate that peak metamorphic temperatures, pre-dating the S_1-shearing, may have exceeded 900°C (Alexejev, 1997).

Younger, generally eastward-dipping, narrow extensional shear zones (S_2) of more local distribution developed both within the tectonic melange zone and the Umba block metasediments. In the latter textural observations show Crd replacing Gar–Sill and suggest strong decompression (Fig. 3b). TWEEQU-calculations for Gar–Sill–Crd–Bt assemblages indicate pressures of 7.5–8.0 kbar and temperatures of 860–840°C (Alexejev, 1997). Decompression reactions from rocks in the tectonic melange zone include Crd–Opx, Opx–Spr–Crd and Opx–Pl rims around Gar-grains and Crd-rims around Opx–Sill intergrowths. We suggest that the decompression occurred during uplift or tectonic erosion of both

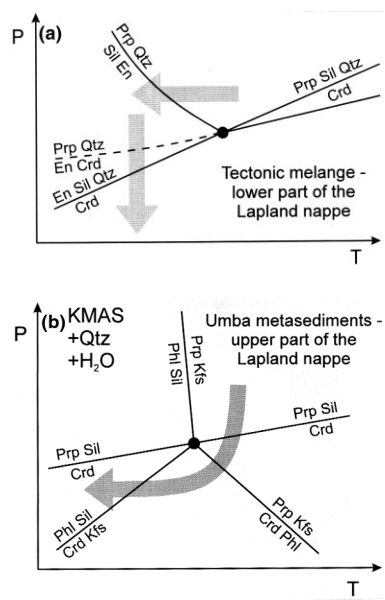

Fig. 3. PT-time cooling paths for (a) the lower part of Lapland nappe (the Tectonic melange zone), and (b) the upper part of the Lapland nappe (Umba metasediments).

the Umba block metasediments and the Poriya Guba series, which had been juxtaposed during the S_1-thrusting. In some places anatectic melting of the rocks occurred along the (S_2) shear zones.

As described above, the southeastern part of the Umba block metasediments is intruded by an enderbite–charnockite suite and a porphyritic granite. The latter is contaminated by sedimentary material and is locally 'crowded' with inclusions of metasediments comparable to the Umba metasediments in the northwest. The *S*-fabric in the enderbite–charnockite suite conforms in orientation with the S_1 shear fabric in the metasediments and those are considered to have developed during the main thrust event which predated local partial melting. Extensional shear zones (S_2) likewise occur in the suite. However, petrography has not revealed any sign of high-grade metamorphism in the enderbite–charnokites. Furthermore, the maximum temperature for homogenization of melt inclusions in thin quartz–feldspar partial melt veins parallel to the mylonitic fabric in the charnockite suite is 750°C at its contact with the Umba block metasediments (Klepinin et al., 1997). This differs significantly from the temperatures (860–840°C) calculated for partially melted metasediments in the Umba block at the contact with the granitoids.

5. Petrology and geochemistry of the Umba igneous suite

The Umba igneous suite (overlapping with the Umba complex of Vinogradov and Vinogradova, 1975) was in the field subdivided into the enderbite–charnockite suite and the porphyritic granite, both occurring in discrete bodies. Both are locally intruded by minor bodies or veins of reddish granite. Of the 19 analyzed samples (Table 1) 17 were collected from the enderbite–charnockite suite (including one sample from a small sill-like body in the Umba metasediments (107174), three from the porphyritic enderbite and charnockite (101248, 107156 and 101249)) and two from the minor bodies of reddish granite (samples 101078 and 107153), united with charnockite suite. Porphyritic granites from the large massif occurred to southeast of Umba were not analyzed.

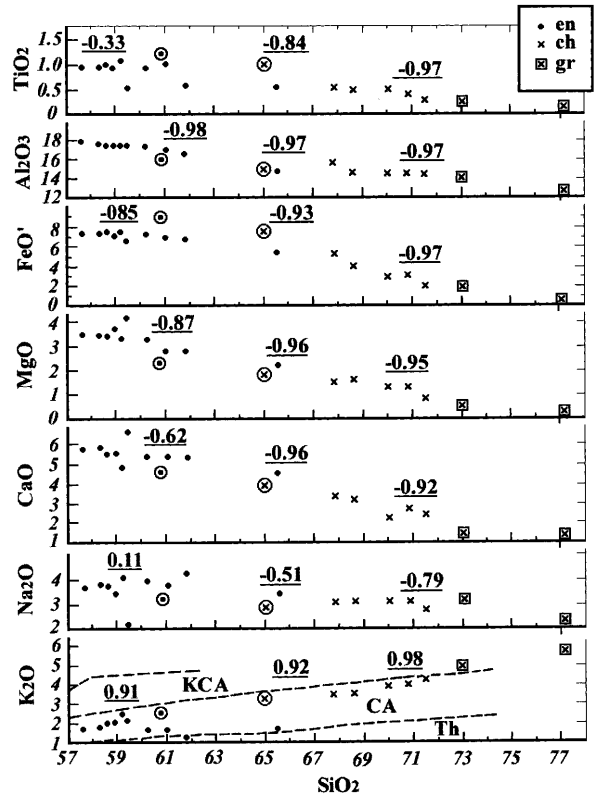

Fig. 4. Harker diagrams for enderbite (en), charnockite (ch), reddish granite (gr); symbols in the circles indicate porphyritic rocks transitional between charnockite and enderbite compositions, one of which was dated. On the diagrams correlation coefficients are written separately for each rock group.

The SiO_2 content in the suite (Table 1) ranges from 57 to 71% with only two samples in the interval 62–67.5%. The late reddish granites show the highest SiO_2 content with values in the range 73–77%. The Umba igneous suite as a whole appears to be discontinuous from plots in Harker's diagrams (Fig. 4). Rocks with less than 2.57% K_2O are defined as enderbites, while those with more than 2.57% K_2O are defined as charnockites. The porphyritic charnockite and enderbite plot in the interval between the two. In the Ab–An–Or diagram (Fig. 5a), most of the enderbite samples plot in the tonalite field (O'Conner, 1965; Barker, 1979), while the charnockites plot near the junction between the granodiorite and granite fields. The porphyritic charnockite and enderbite overlap the two fields, and the late reddish gran-

Table 1
Chemical analyses of enderbites and charnockites

Enderbites											
Analyse	1	2	3	4	5	6	7	8	9	10	11
Samples	107169	107166	107171	107170	107076	107174	107172	101248	101070	1010801	101077
Oxides (*wt.%*)											
SiO_2	57.67	58.35	58.67	58.92	59.11	59.44	60.2	60.82	60.99	61.73	65.48
TiO_2	0.98	0.93	0.98	0.95	1.07	0.5	0.93	1.21	1.09	0.62	0.77
Al_2O_3	17.8	17.9	17.4	17.31	17.59	17.5	17.06	15.98	16.78	16.51	15.58
F_2O_3	6.68	6.49	6.83	6.46	6.46	5.69	6.45	8.28	6.25	6.22	4.77
MnO	0.08	0.07	0.08	0.07	0.08	0.07	0.09	0.11	0.07	0.1	0.06
MgO	3.8	3.66	3.56	3.74	3.34	4.12	3.36	2.19	2.76	2.76	2.29
CaO	5.93	5.87	5.61	5.56	4.75	6.72	5.45	4.44	5.35	5.25	4.52
Na_2O	3.78	3.77	3.82	3.56	4.07	1.95	4.01	3.17	3.79	4.33	3.67
K_2O	1.76	1.73	1.82	1.83	2.47	2.13	1.64	2.42	1.59	1.11	1.54
P_2O_5	0.31	0.29	0.32	0.31	0.3	0.29	0.29	0.44	0.35	0.15	0.23
LOI	0.37	0.24	0.49	0.44	0.25	0.7	0.25	0..44	0.59	0.93	0.38
Total	96.36	99.49	99.75	99.36	99.63	99.37	99.87	99.71	99.73	99.81	99.41
Trace elements (*ppm*)											
Rb	47.7	43.8	56.6	56.2	70.4	81.8	44.2	71.3	50.4	44	48.8
Ba	881	827	742	955	536	1541	560	1303	621	285	543
Pb	6	7	9	7	9	21	8	14	8	11	7
Sr	639	666	614	666	417	817	493	237	487	261	506
La	18	20	32	18	40	27	30	33	26	27	25
Ce	36	43	66	42	76	62	61	69	56	55	41
Nd	22	25	34	23	33	32	33	33	27	24	19
Y	20	19	25	18	13	12	24	32	17	24	9
Th	0	0	1	1	1	9	1	2	1	10	0
Zr	175	170	198	167	149	120	181	311	201	140	125
Nb	8	8.9	9.1	6.9	7.6	5.3	7.5	17.6	8.6	9.2	5.3
Zn	94	84	93	85	86	67	80	115	95	77	65
Cu	31	23	25	24	22	42	21	115	20	13	8
Co	20	19	18	18	19	23	15	19	15	22	12
Ni	35	33	32	35	33	45	33	16	23	51	19
Sc	19	22	20	17	15	21	28	23	18	13	9
V	142	135	136	131	104	142	121	151	138	74	100
Cr	80	75	72	79	73	125	73	38	56	38	37
Ga	23	23	23	21	22	19	20	22	23	18	19
K/Rb	306	329	267	270	291	216	308	282	262	209	262
Rb/Ba	0.054	0.053	0.076	0.059	0.169	0.053	0.079	0.055	0.081	0.154	0.09
Rb/Sr	0.073	0.066	0.092	0.084	0.169	0.100	0.090	0.301	0.103	0.168	0.096
Rb/Zr	0.272	0.256	0.286	0.336	0.472	0.682	0.244	0.229	0.251	0.314	0.390
Ba/Sr	1.38	1.24	1.21	1.43	1.28	1.89	1.13	5.50	1.27	1.09	1.07
K/Ba	16.57	17.41	20.35	15.92	38.25	11.41	24.28	15.43	23.57	32.28	23.57
Ga/Al′	2.44	2.42	2.49	2.29	2.36	2.05	2.21	2.60	2.59	2.06	2.30
Al[a]	0.94	0.96	0.95	0.97	0.98	0.99	0.94	1.01	0.95	0.93	0.99

Table 1 (*Continued*)

Charnockites									Average compositions			
Analyse	12	13	14	15	16	17	18	19	enderbites (10)	chrnockites (7)		
Samples	101249	101246	101071	107156	101247	107167	107153	101078	X	σ	X	σ
Oxides (*wt.%*)												
SiO_2	64.92	67.71	68.61	69.96	70.80	71.47	73.03	77.25	60.06	2.27	71.26	3.18
TiO_2	1.00	0.60	0.54	0.55	0.43	0.31	0.25	0.06	0.88	0.19	0.39	0.18
Al_2O_3	14.81	14.89	14.67	14.56	14.26	14.25	13.97	12.15	17.14	0.70	14.11	0.92
F_2O_3	6.73	4.56	3.66	2.88	2.81	1.97	1.65	0.25	6.23	0.60	2.54	1.41
MnO	0.08	0.05	0.06	0.03	0.03	0.01	0.04	0.01	0.08	0.01	0.03	0.02
MgO	1.65	1.47	1.59	1.34	1.31	0.88	0.48	0.12	3.34	0.57	1.03	0.55
CaO	3.64	3.33	3.18	2.19	2.73	2.47	1.33	1.02	5.50	0.62	2.32	0.88
Na_2O	2.78	3.17	3.19	3.28	3.14	2.88	3.28	2.29	3.68	0.64	3.03	0.35
K_2O	3.36	3.64	3.55	3.99	3.9	4.36	4.8	5.79	1.76	0.36	4.29	0.79
P_2O_5	0.31	0.23	0.18	0.20	0.13	0.11	0.11	0.02	0.28	0.60	0.14	0.07
LOI	0.11	0.11	0.18	0.51	0.20	0.36	0.41	0.27	0.46	0.22	0.29	0.14
Total	99.61	99.76	99.61	99.63	99.89	99.55	99.41	99.53	99.40	0.23	99.62	0.16
Trace elements (*ppm*)												
Rb	77.8	89.9	86.3	121.4	75	94.2	148	139.7	54.4	12.6	107.8	28.5
Ba	1376	1441	1169	934	1007	4224	346	2323	749	341	1635	1290
Pb	20	10	11	20	11	10	21	11	9	4	13	5
Sr	206	433	418	316	361	587	118	470	557	156	386	146
La	48	21	21	24	25	17	17	8	26	7	19	6
Ce	94	38	39	50	43	29	34	11	54	13	35	12
Nd	44	19	18	24	17	15	15	5	27	5	16	6
Y	36	10	11	16	5	4	26	11	18	5	10	8
Th	13	0	0	8	0	0	6	0	2	4	2	3
Zr	298	129	119	152	98	80	76	45	162	28	100	36
Nb	16.7	4.8	4.6	9.6	2.9	1.4	4.1	1	7.6	1.4	4.1	2.9
Zn	98	52	52	44	47	32	29	7	82	11	38	16
Cu	98	13	6	11	47	8	6	5	23	9	14	15
Co	13	9	9	8	9	6	4	4	18	3	7	2
Ni	12	16	12	12	12	10	5	3	34	9	10	4
Sc	18	6	10	6	5	3	4	0	18	5	5	3
V	97	78	64	65	53	52	22	13	122	23	50	24
Cr	30	153	26	30	23	15	9	3	71	25	37	52
Ga	21	18	17	16	15	12	16	9	21	2	15	3
K/Rb	358	336	434	273	432	384	269	344	272	38	340	58
Rb/Ba	0.056	0.062	0.074	0.130	0.074	0.022	0.423	0.060	0.081	0.034	0.121	0.137
Rb/Sr	0.378	0.208	0.206	0.384	0.208	0.160	1.25	0.297	0.105	0.036	0.387	0.387
Rb/Zr	0.261	0.697	0.725	0.799	0.765	1.177	1.947	3.104	0.340	0.137	1.316	0.905
Ba/Sr	6.68	3.33	2.79	2.95	2.79	7.20	2.93	4.94	1.38	0.28	3.85	1.66
K/Ba	20.28	20.96	25.15	35.44	32.17	8.57	115.03	20.70	21.9	8.0	36.9	35.6
Ga/Al′	2.67	2.28	2.19	2.07	1.98	1.59	2.16	1.40	2.32	0.19	2.13	0.32
Al[a]	0.99	0.98	0.98	1.06	1.01	1.01	1.08	0.88	0.96	0.02	1.00	0.06

[a] The numbers of samples used for calculation of the elements average contents are put in brackets. Because of the large deviations of the trace element contents in samples 8 and 12 they were not used for average composition calculations. $Al' = Al_2O_3/(CaO + Na_2O + K_2O)$, $Ga/Al' = Ga/Al \times 10\,000$. The analyses were done in lab of Copenhagen University.

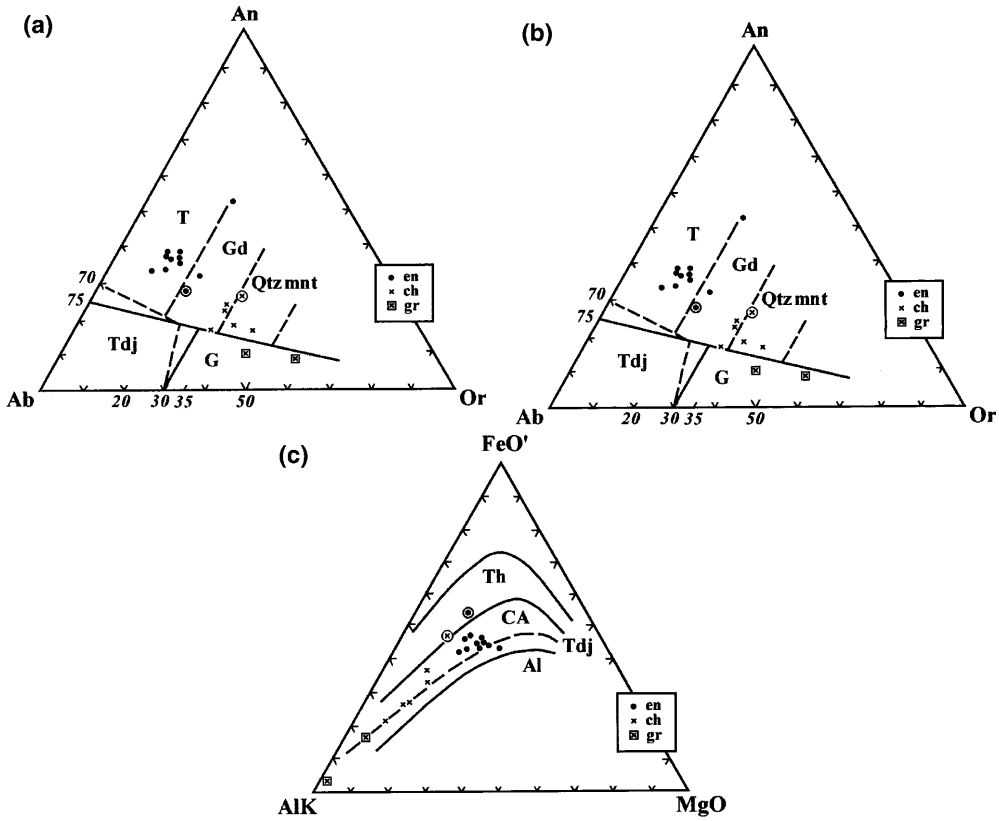

Fig. 5. Enderbite, charnockite, and reddish granites plotted in Ab–An–Or (a), Ab–Otz–Or (b) and Alk-FeO' ($FeO + Fe_2O_3$)–MgO (c) diagrams. Abbreviations. a: T, tonalite; Gd, granodiorite; Qtzmht, quartz monzonite; Tdj, trondhjemite; G, granite; b: Tdj, trondhjemite; CA, calc–alkaline trend; c: Th, tholeiite; CA, calc–alkaline; and Al, alkaline fields; Tdj, trondhjemite trend. The legend is the same as in Fig. 4.

ites plot in the granite field. The K_2O–Na_2O diagram (Fig. 6) shows a similar distribution of rock types. Enderbite points occupy an area in the tonalite field, while the charnockites and granites show a distinct trend parallel to the K_2O axis. The diagram shows that apart from one late reddish granite sample the Umba igneous suite as a whole belongs to I-type granitoids of Misra and Sarkar (1991). In the Ab–Qtz–Or diagram (Fig. 5b), the enderbite points show a trondhjemitic trend (Barker and Arth, 1976), while the charnockites concentrate near the calc–alkaline line, somewhat displaced toward the Ab–Qtz side. Also in the Alk–FeO–MgO diagram (Fig. 5c), the division into enderbites and charnockites can be observed, with the former plotting near trondhjemite trend and the latter occupying the area above this line (Kuno, 1968). The value $Al_2O_3/(CaO + Na_2O + K_2O) = 0.93–0.99$ for the enderbites and 0.98–1.08 for the charnockites (Fig. 1) classifies the suite as alumina granitoids (Chapel and White, 1974).

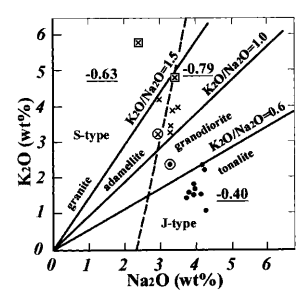

Fig. 6. K_2O–Na_2O diagram. The legend is the same as in Fig. 4.

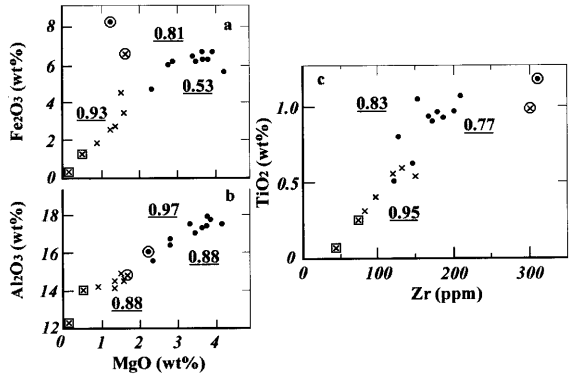

Fig. 7. Correlation diagrams between Fe_2O_3' (total Fe recalculated to Fe_2O_3) and MgO, Al_2O_3 and MgO, and TiO_2 and Zr. Significant correlation coefficients are indicated on the diagrams.

In Harker diagrams (Fig. 4), the Umba igneous suite is as a whole characterized by a strong positive correlation between SiO_2 and Ti, Al, Fe, Mg, Mn, Ca, a weaker positive correlation with Na, and a negative correlation with K. This agrees with the lower average content of Si and K, and the higher content of mafic elements, Ca and Na in enderbites compared to charnockites in Table 1. The distinct trends for most major elements in the Harker diagrams indicate that the enderbites and charnockites belong to one continuous igneous series. Alternatively, they may have originated from mixing of magmas from two different sources. These possibilities for magma genesis may be evaluated further by analysis of correlation between major and trace elements contents and consideration of the gaps in the trends for Na–Si and Ca–Si in Fig. 4, and for Fe–Mg, Al–Mg Ti–Zr in Fig. 7.

Compared to the charnockites, the enderbites show in general a much lower number of correlation coefficients both for major and trace elements. While the charnockites show the same number of correlations as the Umba igneous suite as a whole, the enderbites show a different number of correlations between Ti, Ca, Na and K versus Si, and between combinations of specific trace elements with each other and with Si (Figs. 7–9). For the enderbites, nine significant correlation coefficients between major elements are

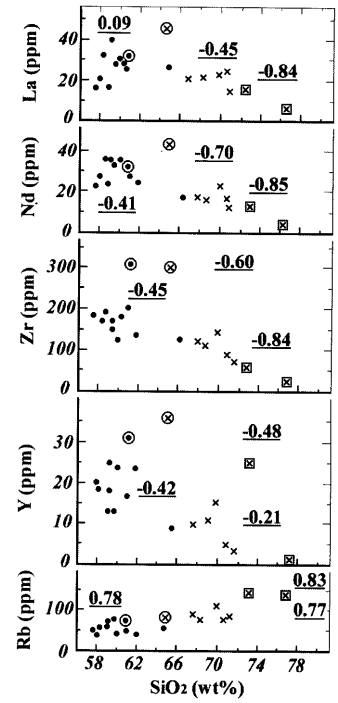

Fig. 8. Correlation diagrams between La, Nd, Zr, Y, Rb and SiO_2. Significant correlation coefficients are indicated on the diagrams.

found out of 55 possible (15%), while 77 correlation coefficients out of 435 possible (18%) are significant between all analyzed elements, including light REE. For the charnockites, the corre-

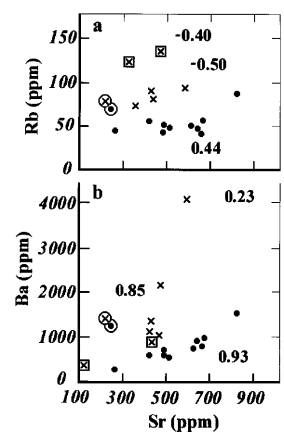

Fig. 9. Correlation diagrams between Rb, Ba and Sr. Significant correlation coefficients are indicated on the diagrams.

Table 2
Correlation coefficients (r) for some elements (r) in enderbites ($n = 10$) and charnockites ($n = 7$)[a]

	End	Charn.		End	Charn.		End	Charn		End	Charn.
Si–La	0.09	*−0.84*	Ti–La	0.10	*0.87*	Fe–La	0.04	*0.78*	Mg-La	0.18	*0.87*
Si–Ce	−0.13	*−0.81*	Ti–Ce	0.05	*0.86*	Fe–Ce	0.21	*0.74*	Mg-Ce	0.06	*0.82*
Si–Nd	−0.42	*−0.90*	TI–Nd	0.11	*0.90*	Fe–Nd	0.42	*0.78*	Mg-Nd	0.40	*0.83*
Si–Zr	−0.45	*−0.86*	Ti–Zr	*0.77*	*0.95*	Fe–Y	*0.74*	0.16	Mg–Zr	0.10	*0.87*
Si–Rb/Zr	0.12	*0.96*	Ti–Nb	0.45	0.68	Fe–Zr	*0.72*	*0.84*			
Ca–La	0.38	0.71	P–La	−0.02	*0.80*	Fe–Nb	*0.75*	0.50	Zr–La	−0.06	*0.83*
Ca–Ce	−0.08	0.60	P–Ce	0.06	*0.89*				Zr–Ce	0.03	*0.88*
Ca–Nd	0.25	0.67	P–Nd	0.38	*0.90*	K–Rb	*0.78*	*0.77*	Zr–Nd	0.24	*0.94*
Ca–Zr	0.04	0.68	P–Zr	0.63	*0.94*	Sr–Ba	*0.92*	*0.85*	Zr–Nb	*0.87*	*0.68*
Ca–Sr	*0.74*	0.34	P–Ca	0.29	*0.80*	Rb–Ba	0.65	−0.18	Zr–Y	*0.88*	0.31
						Rb–Sr	0.44	−0.50	Y–Nb	*0.78*	0.57
Cr–V	0.68	0.67	Mg–Co	0.63	*0.96*	Fe–Co	0.37	*0.88*			
Cr–Co	0.54	0.54	Mg–Ni	0.44	*0.94*	Fe–Ni	0.29	*0.95*	Si–Co	−0.58	*−0.86*
Ni–Co	*0.90*	*0.93*	Mg–Sc	0.65	*0.88*	Fe–Sc	0.55	*0.88*	Si–Ni	−0.36	*−0.94*
Ni–V	−0.23	*0.98*	Mg–V	0.67	*0.94*	Fe–V	0.33	*0.93*	Si–Sc	−0.62	*−0.86*
Ni–Cr	0.35	0.71	Mg–Cr	*0.90*	0.51	Fe–Cr	0.21	*0.73*	Si–V	−0.60	*−0.95*
Co–V	0.04	*0.91*							Si–Cr	−0.62	−0.63

[a] The values of r significant with a probability of 95% are shown in italic, n means number of samples.

sponding correlation numbers are 34 (62%) and 135 (31%), respectively. The differences in the correlations mentioned above for the major elements and for the trace and light rare earth elements in particular are very typical for the enderbite–charnockite suite, and will discussed in more detail in the following.

First of all, the differences in trace element content between two groups must be noted (Fig. 1). Compared to charnockites, the enderbites show higher concentrations of La, Ce, Nd, Y, Th, Zr, Nb, Zn, Cu, Sr, Co, Ni, Sc, V, Cr and Ga, and lower concentrations of Ba, Rb and Pb. The two samples of porphyritic charnockites (101248 and 101249 in Table 1) differ significantly from the others in trace element content (Table 1) and were therefore excluded from the average and correlation coefficient calculations suggesting they are of different magma origin. From the calculations above based on Harker and other diagrams it appeared that the largest number of significant correlation coefficients could be established for the charnockites. These consist of negative correlations between La, Ce, Nd, Zr, Co, Ni, Sc, V, Cr, Ga and Si, positive correlations between Co, Ni, Sc, V, Cr and Mg, Fe, V, Cr, and between Ni, Co and V (Table 2), which usually are lacking for the enderbites. These correlations for charnockites may be explained by fractional crystallization of biotite and feldspars. The positive correlations of P with Ca, La, Ce, Nd, Zr, of Zr with La, Ce, Nd, and of LREE with Mg in the charnockites seem to be caused by the fractional crystallization of monazite, zircon and apatite, during formation of early mafic magma varieties. In contrast, almost none of these correlations were observed for the enderbites, which therefore are suggested to have a different evolution.

From the analyses above it may be concluded that the charnockite group is more strongly differentiated than the enderbite group. The regularities shown by the major and trace elements allow us to suggest that magmatic differentiation under control of K-feldspar fractionation occurred, which is supported by the Ba–Sr and Rb–Sr diagrams (Fig. 9). Furthermore, it would be tempting to suggest that crystallization of the charnockites occurred from residual melts that were formed and separated from the enderbite magma, a suggestion which appears to be supported by the decrease of mafic elements, Zr, Nb, and LREE, and the increase of Si, K, Rb content and Rb/Sr, K/Rb, K/Ba ratios. However, the following does not support such a conclusion

1. Ba shows an inconsistent behavior by increasing in the charnockites.
2. Ba and Sr, not being connected in the correlation, form two independent positive trends in each group (Fig. 9), which can be explained by biotite and/or K-feldspar fractionation.
3. There is a positive correlation of K/Rb ratio with Si.
4. A common trend for Ca–Si, Na–Si, Mg–Fe, Ti–Zr is missing.
5. There is a decreasing Ga/Al ratio and Nb content in the enderbite–charnockite suite as a whole.

All these facts lead to the conclusion that the enderbite–charnockite suite was not co-magmatic, and that the charnockites came from a different source, formed at a deeper level than the enderbites as judged from the very high K/Rb ratio exceeding the values known in crust rocks.

The porphyritic charnockite sample which was used for zircon separation (sample 101249 in Table 1) plots together with the most mafic part of charnockite series, and was distinguished on all the diagrams. It is characterized by extremely high Mg, Fe, Ti, Ca and Ni, Sc, Co, V, Cr contents, but is not exceeding the contents of these elements in the enderbites. At the same time La, Ce, Nd, Zr, Nb, Cu contents are significantly higher than in the charnockites, and even in the enderbites. Its Rb, Ba, Sr and Pb content is similar to that in the charnockites. The porphyritic charnockite sample (101248 in Table 1), associated with the enderbites (see e.g. Fig. 4), is also anomalous and plots in a similar way as sample 101249 in the diagrams. Both samples are metamorphosed and enriched in monazite, zircon, orthite and apatite. The specific geochemical characteristics and field occurrence of the porphyritic granite suggest that it belongs to yet a separate magmatic unit in the Umba igneous suite. Late reddish granites seem not to have solidified under granulite facies conditions (no Opx), and can therefore hardly belong to the enderbite–charnockite suite. They seem to be syn-collisional igneous rocks.

In order to evaluate the tectonic setting in which the magmas were formed further, the rocks of the Umba igneous suite have been plotted in the Nb–Y diagram of Pearce et al. (1984), where

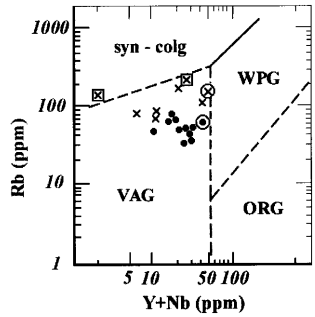

Fig. 10. Rb via Y + Nb diagram (Pearce et al. (1984). Sin-collision granites, VAG, volcanic arc granites; WPG, within-plate granites; ORG, oceanic ridge granites.

the suite plots in the arc- or collision-type granitoid field. In the Rb − (Y + Nb) (Fig. 10), Rb–Si and Rb/Zr–Si diagrams (Pearce et al., 1984), it occupies the arc-type granitoid field. The porphyritic granite plots at the boundary to the within plate field while the late reddish granites plot at the boundary to the syn-collision field. On the (6Ca + 2Mg + Al)–(4Si-11(Na + K)–2(Fe + Ti)) diagram (Fig. 11; Batchelor and Bowden, 1985) the eight enderbite samples plot in the field of pre-plate collision granites of which two are situated near the field of syn-collision granites. Nine samples of the inferred slightly later formed charnockites also plot in the pre-plate collision field and the last two similar to syn-collisional granitoids. The plots in all the diagrams strongly suggest that the enderbite–charnockites of the Umba igneous suite were formed during subduction of oceanic lithosphere in an island arc envi-

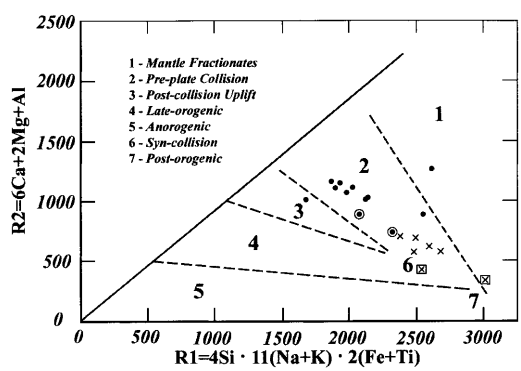

Fig. 11. R1–R2 diagram (Batchelor and Bowden, 1985).

ronment, but porphyritic granites and the reddish granites, both or at least the latter formed in a syn-collisional setting during continent–continent collision that also produced the main thrusting event. The new geochemical data based on our new subdivision of the suite also indicate that its Palaeoproterozoic granitoids have a juvenile character. This conclusion is in good agreement with new Sm–Nd data on the Umba enderbite–charnockite–porphyritic granite suite yielding TDM model ages ranging between ca 1.9 and 2.1 Ga (Timmerman and Balagansky, 1994).

6. U-Pb zircon geochronology of the porphyritic charnockite

6.1. Analytical techniques

Conventional analyses of zircons from sample 101249 were carried out at the Institute of Precambrian Geology and Geochronology, Russian Academy of Sciences (IPGG RAS), St Petersburg, Russia) on a Finnigan MAT 261 8-collector mass-spectrometer in static mode.

Zircons were extracted from the crushed rock sample with heavy liquid and magnetic separation techniques. Hand picked aliquots of zircon were analyzed following the method of Krogh (1993). An air-abrasion treatment of the zircon was performed by the Krogh (1982) technique. All samples were spiked with a 235U-208Pb mixed tracer. The total blanks were 0.05–0.1 ng Pb and 0.005 ng U. The PbDat and ISOPLOT programs by Ludwig (1991a,b) were used for uncertainties and correlations of U/Pb. Ages were determined using the decay constants given by Steiger and Jaeger (1977). All errors are reported at the 2ς level. The error of the U/Pb ratios is 0.6%. Corrections for common Pb were made using values of Stacey and Kramers (1975).

The back-scattered electron imaging (BSE) was taken at the Institute of Precambrian Geology and Geochronology with a SEM (model ABT 55) using an accelerating voltage of 20–30 kV. The BSE images were recorded using the image-analyses system VideoTest-Morpho.

6.2. Analytical results

Inspection of the zircon grain concentrate from sample 101249 led us to distinguish four groups of magmatic zircons that are characterized by the different degrees of progressive recrystallization under high-grade conditions

Type I — Brown-pink turbid subhedral crystals of prismatic shape. The range of crystal sizes is 80–550 μm with a length/width ratio of 2.0–4.0. Growth zoning is visible. The outer parts of the crystals are unzoned and fractured and represent apparently irregular thin overgrowths (Fig. 12 a, b, c). This type of zircon represents about 15% of the bulk population and appears to be of primary igneous origin.

Type IIa — Brown-pink transparent or translucent prismatic or short prismatic zircons, 70–500 μm long with length/width ratio of 2.0–3.0. These zircons reveal complex internal relations that were recognized by using the back-scattered electron imaging techniques (Fig. 12 d, e). They consist of an igneous core with multiple growth zones and an unzoned fractured rim. This zircon type forms about 30% of the population.

Type IIb — Brown-pink transparent or translucent more elongated zircon crystals than the type I crystals (70–500 μm long with length/width ratio of 5.0–6.0) that are characterized similar internal structure (Fig. 12 f, g). The oscillatory zonation of igneous cores is weak. The total amount of these zircon grains is about 30%.

Type III — Pale pink zircons that are transparent and subhedral with an isometric or short-prismatic habit. Generally these zircons do not reveal any internal features, except for the rare traces of zoning (Fig. 12 h, i). It seems that these grains are recrystallized to different degrees from type I and type II zircons. The range of crystal sizes is 60–350 μm with a length/width ratio of 1.0–1.7.

Four multigrain fractions of all recognized zircon types were analyzed (Nos. 1–4, Table 3). Then zircons from the distinct types were subjected to air-abrasion treatment whereby different amount of zircon material was removed (Nos. 5–8, Table 3). On a concordia plot all data points are discordant (Fig. 13). The results for

Table 3
U-Pb isotopic data for the zircon from sample 101249 from Umba massif

NN	Fraction size, μm and zircon type	Fraction weight, mg	Concentrations ppm			Isotopic ratios corrected for blank and common Pb[b]				Rho[c]	Age, Ma		
			Pb	U	$^{206}Pb/^{204}Pb$[a]	$^{207}Pb/^{206}Pb$	$^{208}Pb/^{206}Pb$	$^{207}Pb/^{235}U$	$^{206}Pb/^{238}U$		$^{207}Pb/^{235}U$	$^{206}Pb/^{238}U$	$^{207}Pb/^{206}Pb$
1	>150, I	0.67	16.8	46.0	1366	0.1181 ± 3	0.09703 ± 3	5.524 ± 23	0.3392 ± 11	0.82	1904 ± 8.0	1883 ± 6.0	1928 ± 4.3
2	>100, IIa	0.44	101	281	3601	0.1168 ± 1	0.11304 ± 1	5.418 ± 18	0.3364 ± 10	0.95	1888 ± 6.2	1869 ± 5.8	1908 ± 1.8
3	>100, IIb	0.89	94.1	270	6362	0.1169 ± 1	0.09781 ± 1	5.338 ± 17	0.3313 ± 10	0.97	1875 ± 6.0	1845 ± 5.7	1909 ± 1.5
4	100-70,III	0.52	103	291	5714	0.1171 ± 1	0.08982 ± 1	5.448 ± 18	0.3375 ± 10	0.94	1893 ± 6.2	1875 ± 5.8	1912 ± 2.0
5	>150, I,A 80%	0.67	136	389	7536	0.1196 ± 1	0.07495 ± 1	5.579 ± 17	0.3385 ± 10	0.99	1913 ± 5.9	1879 ± 5.8	1949 ± 0.7
6	>100, IIa,A 50%	0.52	79.8	208	780.7	0.1207 ± 1	0.08861 ± 1	5.731 ± 18	0.3444 ± 11	0.99	1936 ± 6.2	1908 ± 5.9	1966 ± 0.9
7	>100, IIb,A 40%	0.80	130	368	6141	0.1169 ± 1	0.09988 ± 1	5.399 ± 17	0.3350 ± 10	0.99	1885 ± 5.9	1862 ± 5.8	1909 ± 0.8
8	100+70,III, A 40%	0.43	112	310	6125	0.1177 ± 1	0.10051 ± 1	5.547 ± 17	0.3418 ± 10	0.99	1908 ± 6.0	1895 ± 5.8	1922 ± 0.8

[a] Measured ratio.
[b] Uncertainties (95% confidence level) refer to last digits of corresponding ratios.
[c] Correlation coefficients of $^{207}Pb/^{235}U$ vs. $^{206}Pb/^{238}U$ ratios; 50% of zircon was removed during the air-abrasion.

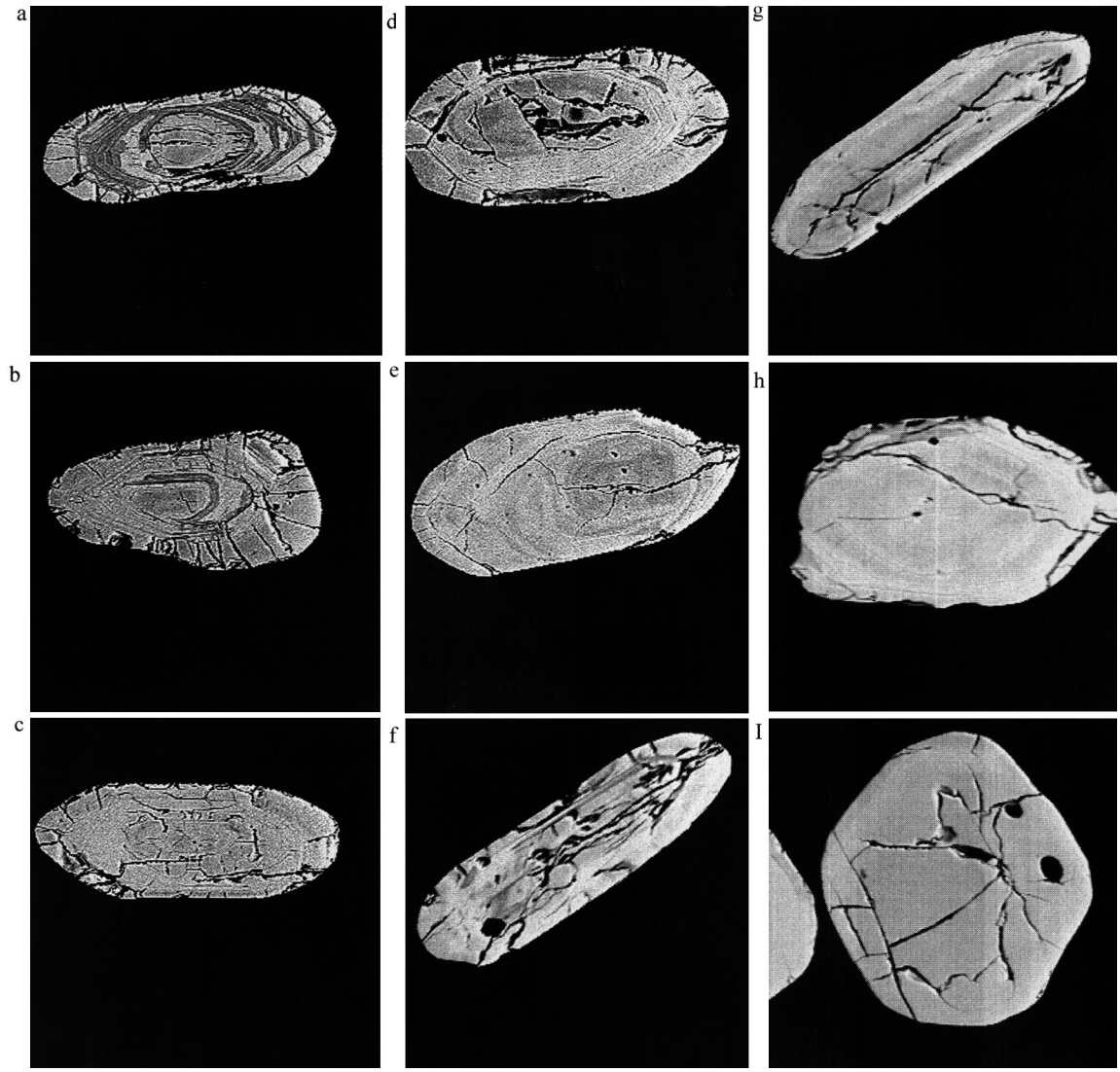

Fig. 12. BSE images of zircons from the Umba porphyritic granite (sample 101249). (a), (b) and (c) — type I zircons; (d) and (e) —type IIa zircons; (f) and (g) — type IIb zircons; (h) and (I) — type III zircons.

unabraded zircons of types IIa, IIb, III were abraded up to 40% (that means 40% of the zircon was removed by abrasion). Type IIb zircons define a discordia which intersects the concordia at 1912.5 ± 7.7 Ma and 187 ± 388 Ma (MSWD = 1.2). The unabraded and strongly abraded zircons of type I and abraded zircons of types IIa and III cluster to the right of the discordia and have older $^{207}Pb/^{206}Pb$ ages (1922 Ma–1966 Ma). The abraded type I and IIa zircons (Nos. 5 and 6, Table 3) are characterized by the oldest $^{207}Pb/^{206}Pb$ ages at 1949 ± 7 Ma and 1966 ± 9 Ma. That is in a good agreement with the morphological features of types I and IIa zircons that show evidence of being the least recrystallized in the population.

We prefer an interpretation of the U–Pb zircon data for the porphyritic charnockite in which the 1912.5 ± 7.7 Ma age, obtained for unabraded zircons of types IIa, IIb, III and abraded type IIb

zircons, represents the intrusion age. The 1949 ± 7 Ma and 1966 ± 9 Ma ages, obtained for abraded type I and IIa zircons, are considered as representing ages of inherited zircons in the magma. This agrees well with field observations that the porphyritic charnockite is vastly contaminated by sedimentary material from the Umba block metasediments. A second possibility for interpretation is that the younger age represents the age of the metamorphism while the intrusion age was older. However, the syn-metamorphic emplacement of the charnockites and the peak metamorphic episode would then have occurred over a period of 40 Ma, as judged from the difference in ages obtained for the igneous cores (abraded type IIa zircons; No. 6 in Table 3) and the upper discordia intercept for recrystallized zircons. This age difference seems too large when compared to the duration of about 20 Ma which is normal for regional metamorphic episodes in areas of polycyclic deformation (Kotov et al., 1995). We therefore strongly prefer that the somewhat older $^{207}Pb/^{206}Pb$ ages of abraded type I and IIa zircons should be explained by the presence of an inherited zircon component that is older than 1920–1930 Ma in the porphyritic granite magma.

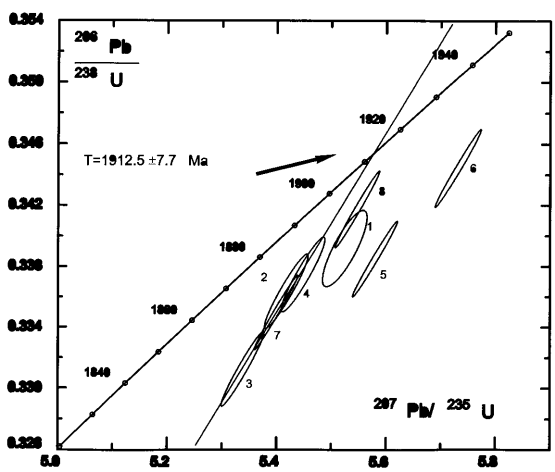

Fig. 13. Concordia diagram for zircons from the Umba porphyritic granite (sample 101249). 1–8 sample fractions: see Table 3 for further information.

7. Discussion and conclusions

The investigation of the Umba igneous complex has revealed that it is composed an enderbite–charnockite suite, including the porphyritic charnockites that in the field area form separate bodies and a porphyritic granite, whose relative age could not be established from mutual relations. Both are intruded by irregular veins or minor bodies of later reddish granite. The rocks of the Umba complex intrude metasediments of the Umba block which also occur as scattered inclusions in the complex. The porphyritic charnockite is locally rich in such xenoliths and contamination by sedimentary material is evident by a minor content of garnet that increases in amount in areas with sedimentary inclusions. Zircon populations from the metasediments show that it was deposited later than 2.1 Ga from sources containing a mixture of Palaeoproterozoic and Archaean material (Bridgwater et al., in press).

The Umba igneous complex and the Umba block metasediments were deformed together during two episodes of deformation. The first one was a major episode of thrusting with the formation of a penetrative shear foliation (S_1), which dips gently eastwards, and a gently SE-plunging lineation. Along with this thrusting, the boundary between the Umba block and the Poriya Guba series in the southeast developed as a strike-slip shear zone, which juxtaposed the two blocks along a tectonic melange zone. The S_1-shearing deformed the enderbite–charnockite suite, and probably also the porphyritic granite, into plate-like, eastward-dipping bodies with concordant boundaries with the surrounding metasediments. While S_1 is well-developed in metasediments forming a strong mylonitic foliation, the rocks of the igneous complex only became well-foliated along their margins due to their more competent character. Predating the shearing, the metasediments underwent high-grade metamorphism and anatexis leading to a high degree of partial melting. This anatexis is also encountered in the enderbite–charnockite suite, but in a much smaller scale and mainly in the marginal parts of the bodies. The second episode of deformation

formed narrow localized extensional shear zones (S_2), which are developed in all rock units.

The S_1-shearing in the tectonic melange zone occurred under high-pressure metamorphism during cooling at constant pressure ($T = 806–818$°C and $P = 9.3–9.5$ kbar (Alexejev, 1997)) and then at decreasing pressure due to tectonic uplift. The enderbite–charnockite suite is assumed to carry primary magmatic orthopyroxene. Though they appear to have suffered by similar deformation events as the metasediments, they do not show signs of high-grade granulite facies metamorphism, possibly because its massive rocks largely formed closed systems during shearing. The S_2-extension occurred under decompression ($P = 7.5–8.0$ kbar and $T = 860–840$°C) (Alexejev, 1997) caused by uplift or tectonic erosion of the thrust pile.

The geochemical investigation of the Umba igneous complex has given important clues for the origin and magmatic evolution of the constituent rocks. Though indistinguishable in the field the enderbite–charnockite suite forms a discontinuous suite with a trondhjemitic trend for the former and a calc–alkaline trend for the latter. Plots of major and trace elements in various diagrams show that the charnockite group is more strongly differentiated than the enderbite group and that magmatic differentiation occurred in the charnockites under control of K-feldspar fractionation. The enderbites, on the other hand, lack differentiation and are considered to have crystallized rapidly from its magma source. The charnockites came from a different source which judging from the high K/Rb ratio formed at a deeper crustal level than the enderbites. Plots (Figs. 10 and 11) show that both members of the enderbite–charnockite suite formed due to subduction in an island arc setting, and Sm–Nd model ages of 2.1–1.9 Ga (Timmerman and Balagansky 1994) indicate in addition that the Palaeoproterozoic suite has a juvenile character.

The studied porphyritic charnockite, which is spatially separated from the enderbite–charnockite suite, occupies compositionally the gap between the enderbite and charnockite groups. However its trace element content and pattern differ significantly indicating that the chrnockites granite come from a separate magma source during collision tectonics.

As presented above, conventional U–Pb zircon dating of the porphyritic charnockite has given discordant ages of 1912.5 ± 7.7 Ma (obtained for unabraded zircons of types IIa, IIb, III and abraded type IIb zircons; Fig. 13), 1949 ± 7 Ma and 1966 ± 9 Ma (obtained for abraded type I and IIa zircons; Fig. 13). There are several possibilities for interpretation of these results. Many zircons may be inherited or contain inherited cores derived from the metasediments, in accordance with the field evidence that the porphyritic charnockite is contaminated by sedimentary material. The type I and IIa zircons (Fig. 13 a–e) have magmatic zoning is seen to overgrow the core, while the outermost thin overgrowth has an unclear origin. These may be overgrown late-magmatic, formed during the cooling of the rocks, or metamorphic, related to the shearing. Since no sign of high-grade metamorphism connected to shearing has been observed in the rocks, we may question if the thin overgrowth could have formed during shearing without any additional heating. The shearing could, however, have caused infiltration of water (and probably K_2O) in the rock, as indicated by replacement of Opx by Bt, which would have created appropriate conditions for zircon growth.

Our preferred interpretation is that the 1912.5 ± 7.7 Ma age represents the age of intrusion, or maximum intrusion age of the porphyritic charnockite and that the 1949 ± 7 Ma and 1966 ± 9 Ma ages for abraded type I and IIa zircons represent ages or mixed ages of inherited zircons from the contaminating Umba block metasediments. The youngest detrital zircons in these metasediments have similar ages (Bridgwater et al., in press). Their source could have been early magmatic arc intrusives, which were eroded shortly after their formation. If the Umba metasediments were deposited in a magmatic arc setting their initial deformation in an evolving arc may have provided the necessary heat flow for anatexis and high-grade peak metamorphism of the metasediments. Therefore, the intrusions of the enderbite–charnokite suite granite during the later evolution of the magmatic arc could have

post-dated the peak of metamorphism, but still pre-date collision and thrusting leading to tectonic telescoping of the units, and thus explain the lower metamorphic grade in the Umba igneous complex compared to the metasediments. If the 1912.5 ± 7.7 Ma age represents the maximum time of intrusion, the true intrusion age might be slightly younger. Tugarinoiv and Bibikova (1980) suggested that peak of high-grade metamorphism in the Lapland granulite belt further northwest is as old as 1910 ± 60 Ma, but later Frisch et al. (1995) more exactly estimated it 1907 ± 6 Ma. If this age also is valid for the Umba block, it indicates, considering the error limits, that the intrusion of the porphyritic granite occurred close to the metamorphic peak.

Acknowledgements

Bridgwater and Marker thank the Danish Natural Research Council for financial support for the fieldwork. We are grateful to Dr Sergei Bushmin for his successful arrangement of the fieldwork on the Kola Peninsula. Geochemical analyses were carried out at the laboratories of the Geological Survey of Denmark and Greenland (GEUS) and of Geological Institute, University of Copenhagen, both of which are thanked. A thanks also goes to Peter Venslev (University of Copenhagen) for having performed mineral separation. The work is a contribution for the SVEKALAPKO Europrobe project and the INTAS-RFBR project 95-1330 and RFBR project 99-05-65263 which have supported the work.

References

Alexejev, N.L., 1997. Reaction textures in igneous and metamorphic rocks and their bearing to P–T path reconstruction (an example from Kandalaksha-Kolvitsa Belt, Baltic Shield). PhD dissertation extended abstracts. St. Petersburg, 26 p. (in Russian).

Balagansky, V.V., Bogdanova, M.N., Kozlova, N.E., 1986. Structural-metamorphic evolution of the NW Belomorian. Geological Institute of the Kola branch of Acad. Sci. Apatity. 100 p. (in Russian).

Balagansky, V.V., Kozlova, N.E., 1987. Mafic dike complex of Kochinny cape and its relation to the Kolvitsa zone evolution. In: T.N. Ivanova et al. Mafic-ultramafic magmatism of the main structural zone of Kola peninsula. Geological Institute of the Kola Branch of Acad. Sci. Apatity. 117 p. (in Russian).

Balagansky, V.V., Timmerman, M.J., Kislitsyn, R.V., 1994. 2.5–1.9 Ga magmatism, metamorphism and deformation in the southeastern branch of the Lapland granulite belt, Kola Peninsula, Russia. Terra Nova 6 (Suppl 2), 2.

Balagansky, V.V., Timmerman, M.J., Kislitsyn, R.V., Daly, J.S., Balashov, Yu.A., Gannibal, L.F., Ryungenen, G.I. and Sherstennikova, O.G., 1998. Isotopic age of the rocks from the Kolvitsa belt and the Umba block (the southeastern extension of the Lapland Granulite Belt), Kola Peninsula. Proceeding Murmansk St. Techn. Univ., N3: 19–32 (in Russian).

Balagansky, V.V., Timmerman, M.J., Kozlova, N.Ye., Kislitsyn, R.V., 1999. A 2.44 Ga old mafic dike swarm in the Kolvitsa Belt, Kola Peninsula, Russia: implication for the early Palaeoproterozoic tectonics in the north-eastern Fennoscandian Shield. Precambrian Research (submitted).

Barbey, P., Convert, J., Moreau, B., Capdevila, R., Hameurt, J., 1984. Petrogenesis and evolution of an early Proterozoic collisional orogenic belt: the Granulite belt of Lapland and the Belomorides (Fennoscandia). Bull. Geol. Soc. Finland 56, 161–188.

Barker, F., 1979. Trondhjemites: Definition, Environment, and Hypotheses of Origin. In: Barker, F. (Ed.), Trondhjemites, Dacites and Related Rocks. Elsevier, Amsterdam, pp. 1–12.

Barker, F., Arth, J.G., 1976. Generation of trondhjemitic-tonalitic liquids and Archaean bimodal trondhjemite-basalt suites. Geology 4, 596–600.

Barling, J., Marker, M., Brewer, T., 1997. Calc-alkaline suites in the Lapland-Kola Orogen, Northern Baltic Shield: Geochemical and isotopic constraints on accretion models. Terra Nova, 9, Abstract Suppl. No. 1: 129.

Batchelor, R.A., Bowden, P., 1985. Petrogenetic interpretation of granitoid rock series using multicationic parameters. Chem. Geol. 48, 43–55.

Bibikova, E.V., Bogdanova, M.N., Skiold, T., 1995a. New U-Pb isotope data for the Archaean in the North-West Belomorian area. Doklady Acad. Nauk. 344, 794–797.

Bibikova, E.V., Slabunov, A.I., Kirnozova, T.I., Makarov, V.A., Kevlich, V.I., 1995b. U-Pb zircon age of the Keret granite-greenstone system in the junction zone between the Karelian and the Belomorian structure of the Baltic shield. Doklady Acad. Nauk. 343, 517–521.

Bibikova, E.V., Skiold, T., Bogdanova, S.V., 1996. Age and geodynamic aspects of the oldest rocks in the Precambrian Belomorian Belt of the Baltic (Fennoscandian) shield. In: Brewer, T.S. (Ed.), Precambrian Crustal Evolution in the North Atlantic Region, pp. 58–68 Geol. Soc. Spec. Publ. N 112.

Bogdanova, S.V., Bibikova, E.V., 1993. The 'Saamian' of the Belomorian Mobile Belt: new geochronological constrains. Precambrian Research 64, 131–152.

Bridgwater, D., Marker, M., Mengel, F., 1991. The eastern extension of the Early Proterozoic Torngat orogenic zone across the Atlantic. In: Wardle, R.J., Hall, J., (eds.), Lithoprobe, Eastern Canadian Shield Onshore-Offshore Transect (ECSOOT), Report No. 27, Memorial University of New Foundland, 76–91.

Bridgwater, D., Scott, D., Balagansky, V.V., Timmerman, M.J., Marker, M., Bushmin, S.A., Alexeyev, N.L., Daly, J.S. (in press). Provenance of early Precambrian metasediments in the Lapland-Kola belt as shown by 207Pb/206Pb dating of single grains of zircon and whole rock Sm–Nd isotope studies. Doklady Acad. Nauk. (submitted) (In Russian).

Chapel, B.W., White, A.J.R., 1974. Two contrasting granite types. Pacific Geol. 8, 173–174.

Daly, J.S., Timmerman, M.J., Balagansky, V.V., Bridgwater, D., Marker, M., 1997. A telescoped passive margin to back-arc transition in the Lapland-Kola Orogen, Northern Fennoscandian Shield. Terra Nova, 9, Abstract Suppl. No. 1, p. 129.

Frisch, T., Jackson, G.D., Glebovitsky, V.A., Yefimov, M.M., Bogdanova, M.N., Parrish, R.R., 1995. U-Pb geochronology of zircon from the Kolvitsa gabbro-anorthosite complex, southern Kola Peninsula, Russia, Petrologiya, vol. 3. MAIK 'Nauka', Moscow, pp. 248–254.

Glebovitsky, V.A., 1993. Tectonics and Metamorphism of Early Precambrian: the Eastern Baltic shield. In: Regionalnaya Geologia I Metallogeniya, vol. N 1, pp. 7–27.

Glebovitsky, V.A., 1997. Early Precambrian of Russia. Harwood Acad. Publishers, 261 p.

Glebovitsky, V.A., Alekseyev, N.L., Dolivo-Dobrovolskiy, D.V. Reaction structures and P-T regimes of the cooling of deep crustal formations of the Kandalaksha-Kolvitsa structural zone 1997. Proceedings of the Russian Mineralogical Society 126 2 1 22 Nauka St Petersburg, Russia

Kaulina, T.V., 1996. Results of U-Pb dating of rock from the Tolstik Peninsula; northwestern region of the White Sea. In: Golubev, A.I., (ed.), Problems of geology of the Karelia and Kola regions, p. 64–71. Rossiyskaya Akademiya Nauk, Karel'skiy Nauchnyy Tsentr. Petrozavodsk, Russian Federation (In Russian).

Klepinin, S., Alexejev, N., Baikova, V.S., Zinger, T.F., 1997. Thermobarometry, Fluid and Melt-inclusions Study for Opx-bearing Granitoid Massifs of the Belomorian Mobile Belt (Baltic Shield, Russia), EUG9, Strasbourg, France. Abstracts.

Korja, T., Tuisku, P., Pernu, T., Karhu, J., 1996. Field, petrophysical and carbon isotope studies on the Lapland granulite belt; implications for deep continental crust. Terra Nova 8 (1), 48–58.

Kozlova, N.E., Balagansky, V.V., Bogdanova, M.N., 1991. Results of a structural and petrological study of the orthopyroxene-sillimanite association in the Lapland Granulites. Izvestija AS URSS Geology 4, 66–75 In Russian.

Kotov, A.B., Kozakov, I.K., Bibikova, E.V., Salnikova, E.B., Kirnozova, T.I., Kovach, V.P., 1995. Duration of regional metamorphic episodes in areas of polycyclic endogenic processes: a U-Pb geochronological study. Petrology 3 (6), 567–575.

Krogh, T.E., 1993. A low-contamination method for hydrothermal decomposition of zircon and extraction of U and Pb for isotopic age determination. Geochim. et Cosmochim. Acta 37, 485–494.

Krogh, T.E., 1982. Improved accuracy of U-Pb zircon by the creation of more concordant systems using an air abrasion technique. Geochim. et Cosmochim. Acta 46, 637–649.

Kuno, H., 1968. Origin of andesite and its bearing on the island arc structure. Bull. Volc. 32, 141–176.

Ludwig K.R., 1991a. ISOPLOT for MS-DOS, version 2.50. U.S. Geol. Survey Open-File Rept. 88–557, 64 p.

Ludwig K.R., 1991b. PbDat for MS-DOS, version 1.21. U.S. Geol. Survey Open-File Rept. 88–542, 35 p.

Marker, M., 1988. Early Proterozoic thrusting of the Lapland Granulite Belt and its geotectonic evolution, northern Baltic Shield. Geol. Fören. Stockholm Förh. 110, 405–410.

Mitrofanov, F.P., Balagansky, V.V., Balashov, Yu A., Dokuchaeva, V.S., Gannibal, L.F., Nerovich, L.I., Radchenko, M.K., Ryungenen, G.I., 1995. U-Pb age of gabbro-anorthosite massifs in the Lapland Granulite Belt. Nor. geol. Unders. 7, 179–183 Special Publication.

Misra, S., Sarkar, S.S., 1991. Linear discrimination among M-, I-, S- and A-granites. Indian J. Earth Sci. 18, 84–93.

O'Conner, J.T., 1965. A classification of quartz-rich igneous rocks on feldspar ratios. US Geol. Surv. Prof. Paper, 525b. pp. 79–84.

Pearce, J.A., Harris, H.B.W., Tindle, A.G., 1984. Trace elements discrimination diagram for the tectonic interpretation of granitic rocks. J. Petrol. 25, 956–983.

Pushkariov, Yu. D., Kravchenko, E.V., Shestakov, G.I., 1978. Principal geochronological stages for Kola peninsula. Nauka 136.

Stacey, J.S., Kramers, I.D., 1975. Approximation of terrestrial lead isotope evolution by a two-stage model. Earth Planet. Sci. Lett. 26 (2), 207–221.

Steiger, R.H., Jaeger, E., 1977. Subcommission of Geochronology: convention of the use of decay constants in geo- and cosmochronology. Earth Planet. Sci. Lett. 36 (2), 359–362.

Timmerman, M.J., Balagansky, V.V., 1994. Tectonic and thermal evolution of the Palaeo-proterozoic Kolvitsa Belt, Kola Peninsula, Russia. Terra Nova 6 (2), 19.

Tugarinov, A.I., Bibikova, E.V., 1980. Geochronology of the Baltic Shield from Zircon Data. Nauka, Moscow, p. 131 In Russian.

Vinogradov, A.N., Vinogradova, G.V., 1975. Geology and petrology of the Umba charnockite to granite complex. In: Batiyeva, I.D. (Ed.), Intrusive Charnockites and Porphyritic Granites of the Kola Peninsula. Apatity, pp. 3–148.